

PCCP

Accepted Manuscript



This is an *Accepted Manuscript*, which has been through the Royal Society of Chemistry peer review process and has been accepted for publication.

Accepted Manuscripts are published online shortly after acceptance, before technical editing, formatting and proof reading. Using this free service, authors can make their results available to the community, in citable form, before we publish the edited article. We will replace this *Accepted Manuscript* with the edited and formatted *Advance Article* as soon as it is available.

You can find more information about *Accepted Manuscripts* in the [Information for Authors](#).

Please note that technical editing may introduce minor changes to the text and/or graphics, which may alter content. The journal's standard [Terms & Conditions](#) and the [Ethical guidelines](#) still apply. In no event shall the Royal Society of Chemistry be held responsible for any errors or omissions in this *Accepted Manuscript* or any consequences arising from the use of any information it contains.

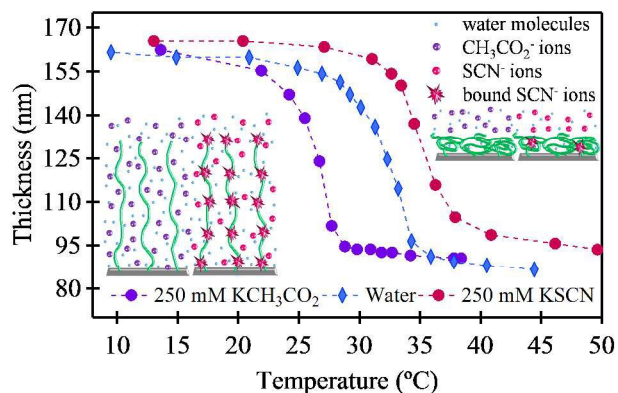
Specific Ion Modulated Thermoresponse of Poly(*N*-isopropylacrylamide) Brushes

Ben A. Humphreys, Joshua D. Willott, Timothy J. Murdoch, Grant B. Webber, Erica J. Wanless

Priority Research Centre for Advanced Particle Processing and Transport, University of Newcastle, Callaghan, NSW 2308, Australia

* corresponding author: erica.wanless@newcastle.edu.au

TOC graphic



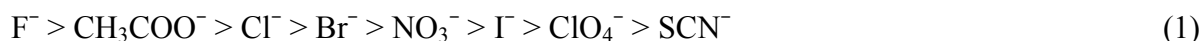
Specific anion identity and concentration dictates the direction and magnitude of the shift in LCST for a pNIPAM brush determined by in situ ellipsometry, QCM-D and static contact angle measurements.

Abstract

The influence of specific anions on the equilibrium thermoresponse of poly(*N*-isopropylacrylamide) (pNIPAM) brushes has been studied using in situ ellipsometry, quartz crystal microbalance with dissipation (QCM-D) and static contact angle measurements between 20 and 45 °C in the presence of up to 250 mM acetate and thiocyanate anions in water. The thickness and changes in dissipation exhibited a broad swelling transition spanning approximately 15 °C from collapsed (high temperatures) to swollen conformation (low temperatures) while the brush surface wettability changed over approximately 2 °C. In the presence of the kosmotropic acetate anions, the measured lower critical solution temperature (LCST) by the three techniques was very similar and decreased linearly as a function of ionic strength. Conversely, increasing the concentration of the chaotropic thiocyanate anions raised the LCST of the pNIPAM brushes with variation in the measured LCST between the three techniques increasing with ionic strength. The thickness of the pNIPAM brush layer was seen to progressively increase with increasing thiocyanate concentration at all temperatures. It is proposed that specific ion binding of the chaotropic thiocyanate anion with pNIPAM amide moieties increases the electrostatic intra- and intermolecular repulsion within and between pNIPAM chains. This allows the brush to begin to swell at higher temperatures and to an overall greater extent.

Introduction

Specific ion effects, which cannot be not wholly explained by classical electrolyte theories, have been extensively investigated ever since they were first observed by Franz Hofmeister in the late 19th century.¹⁻⁵ Initially identified through salt induced variations in the precipitation of egg white protein in aqueous solution, specific ion effects have been found to affect a wide range of phenomena including the stability of colloidal dispersions,⁶ bubbles and foams,⁷ protein solubility,⁸ the response of thermoresponsive polymers (cloud points),⁹ solution properties like viscosity (Dole-Jones Equation),¹⁰ and interfacial properties such as surface tension and ion partitioning.¹¹ Such effects are generally more pronounced for anions than cations due to their greater range in polarisability and follow an approximate trend often referred to as the Hofmeister series.² A general Hofmeister series for monovalent anions is as follows:^{12, 13}



Anions to the left of this series are called kosmotropes while those to the right are called chaotropes with chloride often thought of as the dividing line between the two.² Traditionally kosmotropic ions were classed as water structure makers based on the idea that they enhanced the hydrogen-bonding network in bulk water. Conversely, chaotropic ions were known as water structure breakers as they were thought to disrupt this bulk water hydrogen-bonding network.¹⁴ The widespread popularity of these terms is often misleading and it should be appreciated that they arose from an assumption, rather than an understanding, of their influence.¹² Indeed, although it is accepted that ions can induce changes in the hydrogen bonding pattern of hydration sheath waters, there remains debate regarding the ability of salts to influence bulk water. There is also evidence that ion-partitioning at the air/water and polymer/water interface plays an important role in specific ion effects where it has been reported that larger, less hydrated chaotropic ions have an increased preference for the interfacial region.¹⁵⁻¹⁷ To date, there is no all-inclusive theory that explains specific ion effects within an aqueous system with slight variations in the order of ions, and even complete series reversal reported.^{2, 18}

Poly(N-isopropylacrylamide) (pNIPAM, shown in Figure 1) is an extensively studied neutral thermoresponsive polymer. Free in solution, pNIPAM displays an abrupt and reversible phase transition above its lower critical solution temperature (LCST), which in water lies between 30 °C and 35 °C. The LCST is dependent on polymer concentration, molecular weight and the

type of endgroup present.¹⁹ The behaviour of an aqueous pNIPAM solution is dictated by the enthalpic and entropic interactions between the polymer and surrounding water molecules. Below the LCST the enthalpic contributions (ΔH) dominate and the polymer chains become well-solvated (*i.e.* polymer-solute interactions dominate). However, above the LCST the entropic contributions (ΔS) dominate and the polymer chains collapse into globule conformations. Once collapsed, the pNIPAM chains aggregate via hydrophobic forces and precipitate out of solution (*i.e.* polymer-polymer interactions dominate).²⁰

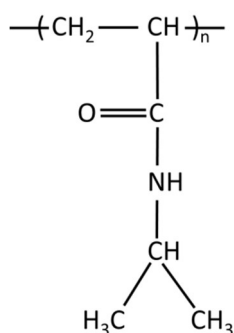


Figure 1. Chemical structure for poly(N-isopropylacrylamide) (pNIPAM).

Like with many other physicochemical and biological phenomena, the behaviour of pNIPAM is influenced by the type of salts present in solution; with specific ion effects following the Hofmeister series.^{3, 4, 9, 21} For most common electrolytes, empirical evidence suggests that varying both the type and concentration of added salt significantly alters the LCST behaviour of pNIPAM, and that the effect of varying the anion is much greater than the cation.⁹ The influence of anions can be explained through three specific interactions with both the polymer and the hydration sheath waters. Firstly, anions can polarise the water molecules that are directly involved in hydrogen bonding with the amide moieties. Here, kosmotropic anions, which have a high charge density and are strongly hydrated, have the largest effect. Anions can also affect the hydrophobic hydration of the pNIPAM chains by altering the surface tension at the hydrophobe (polymer)/water boundary thus affecting the energy required to form clathrate-like water structures at the hydrophobic interface. These effects act to lower the LCST of pNIPAM in a roughly linear fashion with increasing salt concentration.^{4, 9} Weakly hydrated chaotropic anions are known to partition towards hydrophobic surfaces²²⁻²⁶ and the air-water interface.¹¹ They also

have a weak affinity for hydrogen bond donor groups such as amides.^{3,4} These weak interactions are believed to cause the observed initial chaotrope-induced increase in the LCST due to charging of the polymer surface; an electrostatic repulsion which increases the solubility of the polymer.^{3,4} This LCST increase is limited because at higher chaotrope concentrations pNIPAM becomes saturated with anions, and the LCST decreases with more added salt due to increasing dominance of altered hydrogen bonding and surface tension effects.

The temperature sensitive hydration/dehydration response of PNIPAM homo- and co-polymer brushes has attracted attention for a wide range of applications such as chemical sensors,²⁷ attachment-detachment controllable surfaces for living cells²⁸ and proteins,²⁹ chromatography,³⁰ cell culture,³¹ functional composite surfaces,³² and medical diagnostic devices.³³ In order to optimise their usage, however, it is important to understand the detailed behaviour of both the bulk transition and surface response of pNIPAM brushes in various different media. When pNIPAM chains are end-tethered to a surface in the brush regime their behaviour is considerably different to untethered pNIPAM due to increased interchain interactions.^{34,35} These interactions lead to collapse over a significantly broader range of temperatures for thermoresponsive brushes; for pNIPAM brushes, the collapse transition can span up to 20 $\Delta^\circ\text{C}$, as measured by atomic force microscopy (AFM),³⁶ quartz crystal microbalance with dissipation monitoring (QCM-D),³⁶ surface plasmon resonance spectroscopy (SPR)³⁴ and in situ ellipsometry.³⁷ At sufficiently high grafting densities, a vertical phase separation is predicted in which the polymer phase separates into a dense inner region and a well-solvated, dilute outer region at intermediate temperatures. This implies that the surface remains hydrophilic until these outer chains collapse. This is demonstrated experimentally by contact angle measurements that exhibit a narrow LCST transition temperature at about 32 $^\circ\text{C}$, similar to that for free pNIPAM.³⁴

The behaviour of untethered pNIPAM has been extensively studied in different electrolytes, however, the response of end-tethered pNIPAM brushes has received minimal attention. This is especially true in regards to the differentiation of bulk properties and surface effects as a function of both the type and concentration of anions. This current study focusses on the overall response of pNIPAM brushes as observed via ellipsometry and QCM-D measurements as well as the surface response through static contact angle measurements. The brushes were prepared via the 'grafted from' approach using the oxygen tolerant activators regenerated by electron transfer

atom transfer radical polymerisation (ARGET ATRP) technique³⁸ from initiator-functionalised silicon wafers and QCM sensors. Herein, the thermoresponse of pNIPAM brushes was studied as a function of the kosmotropic potassium acetate and chaotropic potassium thiocyanate salts at ionic strengths up to 250 mM.

Experimental

Materials and Chemicals

Native oxide silicon wafers were purchased from Silicon Valley Microelectronics (USA). Quartz crystal microbalance sensors with a 50 nm silica coating (Q-Sense, QSX 303, ~4.95 MHz fundamental frequency) were purchased from ATA Scientific (Australia). Potassium hydroxide (Chem-Supply Pty. Ltd AR grade) was used during sensor and wafer preparation steps. Silane-initiator functionalisation reagents (3-aminopropyl)triethoxysilane (APTES, >99 %), triethylamine (Eth₃N, 99 %) and 2-bromoisobutyryl bromide (BIBB, >99 %) were purchased from Sigma-Aldrich and used as received. The tetrahydrofuran and triethylamine were dried for at least 1 day over 4 Å molecular sieves (ACROS Organics) before use. *N*-isopropylacrylamide (NIPAM, ACROS Organics, 99%) was stored below 4 °C and purified by recrystallisation in hexane prior to use. Polymerisation reagents copper(II) bromide (99.999%), 1,1,4,7,10,10-hexamethyltriethylenetetramine (HMTETA, 97%) and L-ascorbic acid (≥99.0 %) were purchased from Sigma Aldrich and used as received. Ellipsometry, QCM-D and static contact angle experiments were conducted in the presence of aqueous solutions of potassium acetate (Alfa Aesar, >99 %) or potassium thiocyanate (Alfa Aesar, >98 %). The pH of the KCH₃COO and KSCN salt solutions was controlled at pH 5.5±0.1. pH adjustment of the KCH₃COO solutions was made by the addition of acetic acid (glacial acetic acid, Ajax Finechem 100%). The pH of the KSCN solutions was unadjusted. Ethanol (Ajax Finechem, absolute) was distilled before use, methanol (Sigma Aldrich, anhydrous, 99.8 %) was used as received, tetrahydrofuran (THF, Honeywell Burdick and Jackson, >99 %) was dried (for at least one day) over a 4 Å molecular sieve (ACROS Organics) before use and MilliQ™ water (Merck Millipore, 18.2 MΩ·cm at 25 °C) was used throughout.

Surface Initiator-Functionalisation

Cleaned wafers and sensors (see ESI†) were amine-functionalised at room temperature via exposure to APTES vapour at <5 mbar for 30 min before being annealed for a further 30 min in air at 110 °C.³⁹⁻⁴¹ Bromine functionalisation of the APTES layer was then performed by immersion of the wafers and QCM sensors in a solution of BIBB (0.26 mL) and anhydrous triethylamine (0.30 mL) in anhydrous THF (10 mL) under a N₂ atmosphere for 60 min.³⁹⁻⁴¹

Brush Polymerisation via ARGET ATRP

The ‘grafted from’ activators continuously regenerated by electron transfer atom transfer radical polymerisation (ARGET ATRP) method³⁸ was used to synthesise pNIPAM brushes from the surface bound bromine initiator moieties. A typical pNIPAM brush polymerisation was performed in a water/methanol mixture (2:1 v/v) with added NIPAM/CuBr₂/HMTETA/ascorbic acid in the molar ratio of 900/1.5/15/10, while the monomer to solvent mass ratio was 0.05/1. For a more detailed brush synthesis protocol see the ESI†.

Preliminary ellipsometric experiments deemed a dry brush thickness of ~50 nm was ideal due to the highest signal to noise ratio where any changes in the measured data due to brush swelling or collapse are large compared to the noise in the recorded data at equilibrium. QCM and static contact angle measurements were carried out on brushes of similar dry thickness and all experiments for each technique were performed on a single brush to ensure the results obtained were comparable. The measured dry brush thickness values for the three brushes studied are given in Table 1.

Table 1. Dry brush thickness values for the pNIPAM brushes studied.

	Brush thickness^a (nm)
Ellipsometry	56.6 ± 1.4
QCM-D^b	58.6 ± 1.8
Contact angle	44.8 ± 2.5

^aError bars are the standard deviation from several measurements across the brush surface.

^bMeasured for a brush grown on a sister wafer (see ESI†).

Ellipsometric Experiments

Measurements were conducted on a Nanofilm EP3 single wavelength (532 nm green laser) imaging ellipsometer controlled by EP3View software. WVASE32 software was used to model the ellipsometric parameters (Δ and Ψ) with details given in the ESI†. For in situ measurements, a Nanofilm SL fluid cell with optical glass windows was used to house the sample. Only a single angle of incidence was available (60°) since the incident laser must be normal to the cell window. The internal volume of the cell was 0.70 mL and the exposed area of modified wafer was 180 mm^2 . The Δ and Ψ parameters were recorded by employing a script that performed repeated nulling one-zone measurements every 15 s. A multilayer-slab model was employed to each Δ and Ψ pair to determine the solvated brush thickness (see ESI† for more details). The brush was defined as reaching its equilibrium steady state when the brush thickness was constant for a minimum of 20 min. A measured Δ offset of -1.5° , caused by birefringence of the glass windows of the fluid cell was also accounted for in the optical model.⁴²

The temperature controlled experimental solution was pumped at $\sim 4 \text{ mL} \cdot \text{min}^{-1}$ along a minimum length of insulated 1.5 mm internal diameter silicon tubing through the flow cell and copper base plate of the ensemble. This ensured the temperature gradient throughout the pNIPAM brush, wafer and solution within the fluid cell was minimised. A temperature logger (Measurement Computing Co., Data Acquisition USB-TC) measured and recorded the temperature of the solution inside the cell via a K-type thermocouple (maximum error of $0.70 \text{ }^\circ\text{C}$, typical error $0.35 \text{ }^\circ\text{C}$). All experiments were conducted from high to low temperatures ($\sim 50 \text{ }^\circ\text{C}$ to $\sim 10 \text{ }^\circ\text{C}$ inside the fluid cell) to reduce the potential for bubble formation within the cell. This was greater at elevated temperatures with the undesirable consequence of cell disassembly and the experiment having to be restarted. Room temperature water ($\sim 22 \text{ }^\circ\text{C}$) was cycled through the system at $\sim 2 \text{ mL} \cdot \text{min}^{-1}$ overnight ensuring thorough rinsing of pNIPAM brush, flow cell and base plate between measurements. The brush was maintained in the aqueous environment for the duration of the experiment.

Although Zhang has reported that pNIPAM brushes exhibit a temperature direction dependent hysteresis between equilibrium swelling and collapse conformations using QCM measurements, the brushes studied were prepared using the ‘grafted to’ technique from a gold layer where existing polymer chains were grafted onto the surface.⁴³ Studies by Jhon et al. and Varma et al.

were performed on pNIPAM brushes prepared using a similar ‘grafting from’ technique from a silicon oxide layer as employed here.^{44, 45} Notably, both Jhon et al. and Varma et al. have shown that the response of a pNIPAM brush is reversible and displays very little hysteresis between equilibrium swelling and collapse conformations using QCM, and spectral reflectance measurements respectively. The Varma and co-workers study indicated that a brush of similar dry thickness with a comparable swelling ratio displayed a 0.4 °C hysteresis, therefore comparison of LCST values from the three techniques used in this study is considered valid.

QCM-D Experiments

A KSV Z500 quartz crystal microbalance capable of monitoring dissipation (KSV, Finland) was used, with the sensor housed in a parallel flow chamber sealed with an O-ring and clear Perspex window. The internal geometry of the flow cell was cylindrical with a volume of 0.25 mL and a circular exposed area for the brush modified sensor of 154 mm². The QCM technique is sensitive to changes in the solvent retained within or hydrodynamically coupled to polymer brushes.⁴⁶ Oscillations of the QCM sensor at the fundamental resonant frequency (~5 MHz) and higher overtones (~15, ~25, ~35 and ~45 MHz) were measured in this study with frequency ($\Delta f_n/n$) and dissipation (ΔD_n) data for the 3rd ($n = 3$) overtone (~15 MHz) presented herein.

A major challenge facing the use of QCM when studying solvated polymer brushes is separating the frequency response attributable to changes in adsorbed mass or the viscoelasticity associated with the brush. For an elastic rigid film, generally when $|\Delta D_n / (\Delta f_n/n)| < 0.4 \times 10^{-6} \text{ Hz}^{-1}$,⁴⁷ the Sauerbrey equation can be used to extract the areal mass density of the film, which has a contribution from the mass of the solvent entrained within and coupled with the film.⁴⁸ However, as is the case for most soft dissipative films, the Sauerbrey model is not applicable in this instance due to the flexible nature of the solvated brush layer.⁴⁷ Furthermore, the extensive uptake and release of solvent from within the pNIPAM films during swelling and collapse for all conditions results in very large changes in resonant frequency, such that variations between conditions (salt type or concentration) are difficult to ascertain with confidence. Therefore we report changes in dissipation of the pNIPAM layer as an indicator of conformational variations. All ΔD results presented are relative to zero ΔD for each experiment which for simplicity was deemed to be the dissipation value for the equilibrated brush at high temperature, in its collapsed conformation. Owing to the relative nature of the initial zero ΔD value, comparing the absolute

rigidity of the brush in different electrolytes, or even concentrations of the same electrolyte is impossible.

QCM measurements are affected by changes in solution viscosity (which varied as a function of solution temperature),⁴⁹ therefore, the measured dissipation data presented in this study was normalised using the temperature response for a bare sensor. The response of a bare crystal to changes in temperature when immersed in water and 500 mM potassium acetate and thiocyanate were measured where the influence of the added electrolyte was negligible thus all data presented has been normalised against water. Temperature of the experimental solution was controlled by continuous pumping of solution through the cell at $\sim 4 \text{ mL} \cdot \text{min}^{-1}$ with the heat exchange section of the instrument bypassed to reduce temperature losses between the external reservoir and flow cell. The temperature of the solution within the cell was monitored using a temperature logger with a K-type thermocouple positioned through the Perspex window directly above the sensor. All experiments were conducted from high to low temperatures ($\sim 50 \text{ }^\circ\text{C}$ to $\sim 10 \text{ }^\circ\text{C}$ inside the flow cell) and the time that the sample was exposed to elevated temperatures ($>40 \text{ }^\circ\text{C}$) was kept to a minimum. Experiments were conducted from high to low temperature for the same reasons as for the ellipsometry experiments. The brush was defined as reaching its equilibrium steady state when the measured Δf and ΔD results were constant for at least 20 min. A minimum of 100 mL of solution from the next experiment was flowed through the cell at $20 \text{ }^\circ\text{C}$ to ensure complete exchange, if any, of ions within the brush and of solution within the cell and tubing.

Static Contact Angle Experiments

Contact angle experiments were conducted on an OCA20 dynamic contact angle instrument (DataPhysics, Germany). The pNIPAM brush was positioned on Teflon blocks in an inverted orientation and immersed in a temperature controlled solution within a 5 cm^3 optical glass cell. Contact angle experiments were conducted from low to high temperatures, opposite to that for the ellipsometry and QCM-D studies. The sample was allowed to equilibrate for at least 20 min at each temperature prior to capturing a series of five separate captive air bubbles recorded over $\sim 1 \text{ min}$ period. The brush coated wafer was tilted whilst submerged to remove previous bubble. The average for the left and right measured contact angles for each set of five bubbles is reported

with the error reported to be 1 standard deviation. The brush-modified wafer was stored in a vial of water at room temperature between experiments.

Results and Discussion

pNIPAM Brush Synthesis

ARGET ATRP methodology was successfully deployed to synthesise pNIPAM brushes from bromine initiator sites covalently bound to both silicon wafers and silica coated QCM sensors (see Figure S1 in ESI†). This technique ensured a well-controlled synthesis and achievement of target brush thicknesses. PNIPAM brushes of over 150 nm dry thickness (ellipsometry) were prepared via this route within 4 h as shown in ESI† Figure S2. Excellent concordance is seen between the three syntheses shown. It should be noted that since the pNIPAM brushes were synthesised using the same surface-bound initiator approach, variations in the grafting density should be minimised, thus limiting the significant effects this can have on the thermoresponse of pNIPAM brushes.⁵⁰

Thermoresponse of pNIPAM Brushes in Pure Water

Figure 2 shows the equilibrium hydration transition of a pNIPAM brush in pure water as a function of temperature between 10 °C and 45 °C via ellipsometry (Figure 2a), QCM-D (Figure 2b) and static contact angle (Figure 2c) measurements. For this comparative study all three brushes were polymerised under identical conditions to minimise any variations in dry thickness, chain dispersity and grafting density between each pNIPAM brush studied; see Table 1. Sigmoidal curves were fitted to each data set (red dashed lines) using Equation 1 (see ESI† Figure S3 for a sigmoidal fit example showing all parameters and Table S1 for all parameters for each experiment):

$$y = A + \frac{B}{1 + \exp(k(T_0 - T))} \quad (1)$$

where y is the measured parameter (i.e. thickness, dissipation or contact angle) as a function of temperature, T . The constant A represents the plateau value of the given parameter at low T , and B is the change in this parameter to the plateau value at high T . The value T_0 represents the temperature at which the parameter has changed by 50%, and is used here as a measure of the LCST. The constant k (with units of T^{-1}) is the steepness of the curve during the transition and correlates with the width of the transition. It is clear that k is related to the rate of change, where the higher this transition rate, the more the measured parameter changes for a given change in temperature. The parameters required to produce these fits are shown in Table 2.

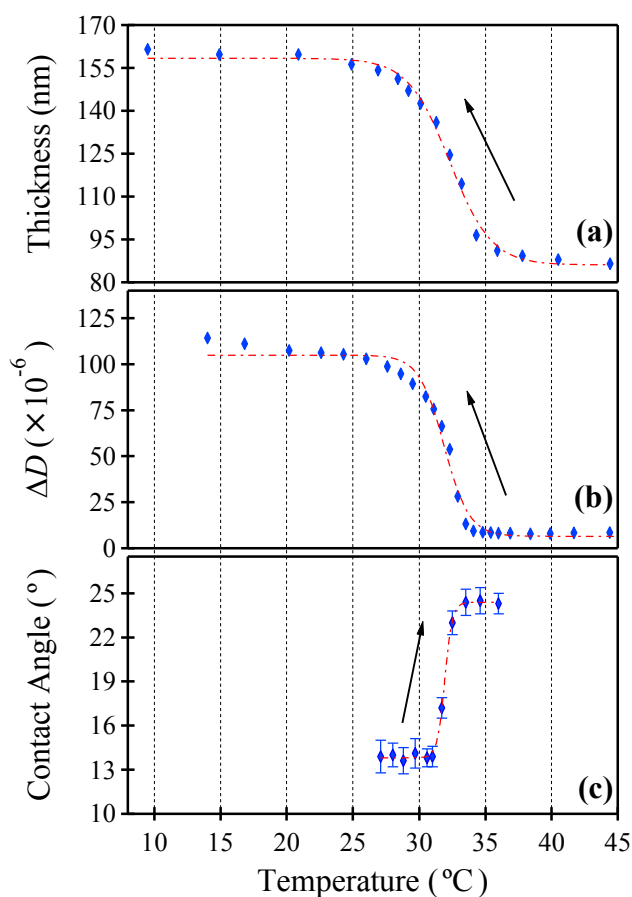


Figure 2. Equilibrium thermoresponsive behaviour of pNIPAM brushes in water as a function of temperature monitored by (a) ellipsometry, (b) QCM and (c) static contact angle. Arrows indicate direction of measurement and error bars display one standard deviation (error smaller than symbols in (a) and (b)).

Table 2. LCST and transition rate for pNIPAM brushes in pure water for equilibrium ellipsometry, QCM and static contact angle measurements (see Table S1 in ESI† for all sigmoidal parameters).

	LCST (°C)	Transition Rate (°C ⁻¹)
Ellipsometry	32.3 ± 0.2	0.63 ± 0.08
QCM ΔD	31.9 ± 0.1	1.0 ± 0.1
Contact Angle	31.9 ± 0.5	3.3 ± 1.1

In situ ellipsometry, QCM-D and static contact angle measurements at equilibrium were utilised in this study with each technique providing insight about the conformation, structure and physical properties of the brush layer. Ellipsometry was a very effective method for determining the average thickness of the pNIPAM brush layer, however, limitations brought about through the use of a slab model for the density profile of the polymer brush layer (i.e. the assumption of constant polymer density) resulted in the ellipsometry measurements being relatively insensitive to chain dispersity. QCM-D measurements yielded information about how effective the pNIPAM brush was at dissipating energy which is directly related to the elasticity/rigidity of the brush layer. Unlike ellipsometry, QCM-D is very sensitive to chain dispersity where even a small fraction of higher molecular weight polymer chains extending further into solution can affect the ΔD measured for the brush layer.⁵¹ All ΔD results reported in this study were for the 3rd overtone ($n=3$). Both ellipsometry and QCM-D monitored bulk pNIPAM properties whereas static contact angle measurements were particularly sensitive to the outermost region of the pNIPAM brush layer. The properties of the periphery of the brush are just as important as the bulk properties as this is the boundary between the polymer brush layer and the external environment. When these three techniques are employed to characterise similar brushes as is the case here, their combined analysis can provide a highly detailed and powerful image of the brush layer as it progresses through its hydration transition.

Equilibrium ellipsometric data (Figure 2a) show that the overall pNIPAM brush thickness changes substantially as a function of solution temperature between ~36 °C (collapsed) and ~21 °C (swollen). Figure 2b exhibits the change in normalised dissipation (ΔD) for the pNIPAM modified QCM sensor as a function of the overlying temperature. The dissipation of the brush is low above ~35 °C indicative of a rigid and collapsed brush, where the polymer chains are

relatively dehydrated and polymer-polymer interactions are dominant. The pNIPAM brush then goes through a broad hydration transition (~ 35 to ~ 22 °C) over which the dissipation increases, corresponding to an increasingly elastic, swollen brush conformation. The brush becomes more elastic throughout its hydration transition due to the polymer chains becoming more flexible as they progressively hydrate and stretch further normal to the surface. The dissipation data returns a similar LCST (31.9 °C) to that found via ellipsometry, however for the QCM-D data the transition rate was higher. This indicates that the hydration transition occurred over a reduced temperature range in the QCM measurement. Static contact angle measurements (Figure 2c) display a distinctly different response. The changes in contact angle occur over a significantly condensed temperature range (~ 2 °C) compared to the broad transitions measured for the ellipsometry and dissipation studies. It is evident that the surface remains more hydrophilic for the majority of the overall dehydration transition of the brush and becomes more hydrophobic just prior to the brush reaching its collapsed plateau. The LCST (31.9 °C) was again very similar to that determined for both the ellipsometry and QCM measurements, and the determined rate was much higher reflecting the fact that the surface wettability transition occurred over a narrow range.

Looking at the equilibrium brush response shown in Figure 2, a detailed insight into the thermoresponse of a pNIPAM brush in pure water can be gained. Firstly, when the response of the bulk brush properties of thickness (Figure 2a) and dissipation (Figure 2b) are examined, it is evident that the brush increases in thickness 1 to 2 °C above that at which any appreciable increase in ΔD is detected. This implies that even though the pNIPAM brush is increasing in thickness, the brush layer remains more rigid. As the temperature is decreased incrementally from high to low, the collapsed pNIPAM brush layer begins to swell normal to the substrate. The bulk hydration transition continues over a broad temperature range with the brush solvation and extension continuing until a steady state is reached at temperatures below about 21 °C. What the contact angle measurements show, however, is that the brush surface reached a more hydrophilic state at much higher temperature ~ 31 °C. These findings are supported by the results of Balamurugan and co-workers who measured a broad hydration transition via SPR spanning approximately 10 to 40 °C, yet a sharp wettability transition was observed at ~ 32 °C.³⁴

Combining the insight gained from the ellipsometry, QCMD and contact angle measurements is powerful. The implications from this study are that as the temperature is reduced, the brush layer extends normal to the surface, starting from the periphery of the brush working its way down towards the substrate. This is evident where the surface of the brush displays a narrow wettability transition beginning at a similar temperature to that measured for the initial increase in brush thickness and dissipation, yet the bulk brush properties continue to change over a broad temperature range well below the temperature at which the surface wettability had attained a plateau.

Specific Ion Effects on the Thermoresponse of pNIPAM Brushes

A previous study of anions including acetate and thiocyanate on the LCST of untethered pNIPAM shows that the expected trends predicted for a Hofmeister series is followed.¹³ Acetate is a kosmotropic anion with low polarisability and a high degree of hydration.¹² The reduction in LCST is approximately linear as a function of concentration.¹³ Thiocyanate on the other hand is a chaotropic anion that is highly polarisable and weakly hydrated.⁵² When thiocyanate ions are present in aqueous solutions with untethered pNIPAM, they affect the LCST in a non-monotonic fashion. At low concentrations of thiocyanate the LCST is slightly increased, before reaching a molecular weight dependent maximum value between approximately 200 to 400 mM; additional increases in thiocyanate concentration then reduce the LCST.^{3-5, 13}

In this study both acetate and thiocyanate anions are paired with the mildly chaotropic potassium cation (K^+), ensuring that any variations in the LCST between the two salts is directly related to the identity of the anion. Experiments were performed in the presence of 10, 100 and 250 mM solutions of potassium acetate and then potassium thiocyanate. All experiments were performed using the same brush (per technique) with copious rinsing with the succeeding solution between measurements.

Figure 3 displays the equilibrium results for the ellipsometry, QCM and static contact angle measurements for pure water together with potassium acetate (a, b and c) and potassium thiocyanate (d, e and f) experiments. The lines represent sigmoidal fits (Eqn. 1) to each respective data set. The acetate experiments in Figure 3 display a clear trend for all three

techniques. Here, the temperature at which the change in brush behaviour is detected shifts to lower temperatures as the concentration of potassium acetate is increased. This trend is predicted for increasing concentrations of the kosmotropic acetate anion, and is comparable to the behaviour of untethered pNIPAM.¹³

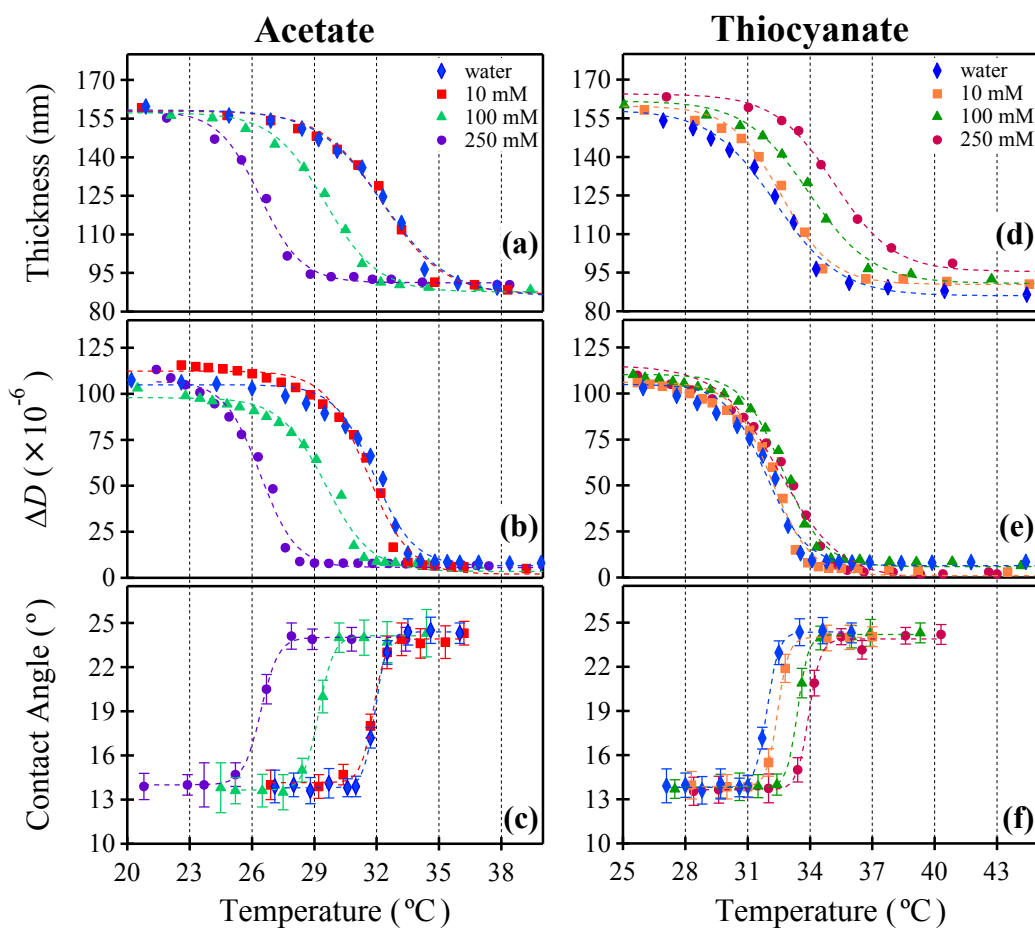


Figure 3. Influence of potassium acetate and potassium thiocyanate on the equilibrium thermo-responsive behaviour of pNIPAM brushes monitored by (a and d) ellipsometry, (b and e) QCM ΔD and (c and f) static contact angle measurements respectively. Error bars display 1 standard deviation (error smaller than symbols for a, b, d and e).

Examining the acetate data in Figure 3a and Table 3, some interesting observations can be made. Firstly, the plateau collapsed and swollen thicknesses of the pNIPAM brush are relatively unaffected by potassium acetate. Furthermore the shape of the thickness transition is similar, though the rate increases with potassium acetate concentration. Here, by increasing the

concentration of acetate ions the temperature range over which the pNIPAM brush swells decreases. This phenomenon hasn't previously been reported for pNIPAM brushes to our knowledge. At high temperatures there is an entropic barrier to the association of water molecules with the pNIPAM which is enhanced by the presence of well-solvated acetate anions. As the temperature is decreased this enthalpic barrier reduces, as the kinetic energy of the water molecules decreases. It is clear that at higher acetate concentrations, the temperature at which this barrier is sufficiently reduced to allow brush swelling decreases. However, once this barrier is overcome the brush attains the equilibrium low temperature thickness over a narrower temperature range.

Table 3. Influence of pure water and 10, 100 and 250 mM solutions of potassium acetate and potassium thiocyanate on the LCST and transition rate of pNIPAM brush response for equilibrium ellipsometry, QCM ΔD and static contact angle measurements (see Table S1 in ESI† for all sigmoidal parameters).

	Ionic Strength (mM)	Acetate		Thiocyanate	
		LCST (°C)	Transition Rate (°C ⁻¹)	LCST (°C)	Transition Rate (°C ⁻¹)
Ellipsometry	pure water	32.3 ± 0.2	0.63 ± 0.08	32.3 ± 0.2	0.63 ± 0.08
	10	32.3 ± 0.2	0.71 ± 0.10	32.6 ± 0.1	0.83 ± 0.07
	100	29.5 ± 0.1	0.83 ± 0.07	33.9 ± 0.2	0.67 ± 0.09
	250	26.4 ± 0.2	1.0 ± 0.1	35.1 ± 0.1	0.71 ± 0.05
QCM ΔD	pure water	31.9 ± 0.1	1.0 ± 0.1	31.9 ± 0.1	1.0 ± 0.10
	10	31.5 ± 0.1	1.0 ± 0.1	32.1 ± 0.1	1.1 ± 0.12
	100	29.5 ± 0.1	1.0 ± 0.1	32.7 ± 0.1	1.0 ± 0.10
	250	26.4 ± 0.1	1.1 ± 0.12	32.5 ± 0.2	0.67 ± 0.04
Contact Angle	pure water	31.9 ± 0.5	3.3 ± 1.1	31.9 ± 0.5	3.3 ± 1.1
	10	31.9 ± 0.5	3.3 ± 1.1	32.4 ± 0.5	3.3 ± 1.1
	100	29.2 ± 0.5	2.5 ± 0.63	33.4 ± 0.5	3.3 ± 1.1
	250	26.5 ± 0.5	2.5 ± 0.63	33.9 ± 0.5	3.3 ± 1.1

The acetate QCM ΔD and static contact angle data also show a reduction in the LCST, though in these two techniques there is no discernible trend in the transition rate of brush swelling or collapse. The LCST values measured by each technique, for each acetate concentration, are remarkably similar. This indicates that the outermost region of the brush is responding to the

added salt in a similar fashion to the overall brush. The implications are that the specific ion effects arising from exposure to acetate ions are acting equally throughout the brush profile.

Figures 3d, e and f show the equilibrium ellipsometry, QCM and static contact angle results for pure water and potassium thiocyanate solutions. The thiocyanate results in Figure 3 show a stark difference to the results displayed for the kosmotropic acetate salt. For the chaotropic thiocyanate, the temperature at the onset of the hydration transition from collapsed to swollen, and the change in wettability, increases with ionic strength. This is expected from the location of thiocyanate within the Hofmeister series and has been reported for untethered pNIPAM at these ionic strengths.³⁻⁵

Along with the different influence on LCST, the ellipsometry data (Figure 3a and d) reveal additional anion dependent behaviours. Firstly, the collapsed and swollen thicknesses of the pNIPAM brush are affected by the presence of the added thiocyanate. The brush becomes increasingly more swollen at all temperatures as a function of potassium thiocyanate concentration. The shape of the thickness transition also changes with potassium thiocyanate concentration. For the 100 mM and 250 mM thiocyanate cases the temperature at which the plateau thickness is reached (at high or low T) is much further from the LCST value than observed for acetate; this is particularly evident for the 250 mM thiocyanate. For the two highest thiocyanate concentrations, the transition is broader, and much more gradual around the plateau values, than in acetate. This is evidence that the thiocyanate anions behave via a different mechanism compared to the acetate anions. Unlike kosmotropes such as acetate, thiocyanate anions have been shown to directly associate with the amide group of pNIPAM.³⁻⁵ Moreover, thiocyanate anions, and chaotropes in general, have been shown to partition towards hydrophobic surfaces.²²⁻²⁶ Direct association of thiocyanate anions with pNIPAM chains within the brushes would result in electrostatic repulsion within and between neighbouring chains owing to the local increase in thiocyanate anion concentration. This would result in the observed thiocyanate concentration dependent swelling of the brush. Interestingly the presence of thiocyanate does not appear to change the rate of the hydration transition.

Unlike the behaviour in potassium acetate, the QCM ΔD results for potassium thiocyanate do not follow the corresponding ellipsometry data. This is increasingly evident for the 100 and 250 mM thiocyanate solutions where the ellipsometry measures a significant increase in the LCST but

QCM does not. The data in Figure 3d and e suggest that during the swelling transition the pNIPAM brush initially increases in thickness (ellipsometry) without changing its stiffness (QCM). This may be due to the partitioning of poorly hydrated thiocyanate ions into the brush causing an electrostatically driven swelling. In this scenario, since the collapsed pNIPAM brush is already behaving as a rigid layer, such short, electrostatically extended rigid sections of the polymer chains would not make any additional contribution to the dissipation. The static contact angle measurements in Figure 3f display a response that is intermediate to ellipsometry and QCM measurements; contact angle is dependent on thiocyanate concentration but not as much as ellipsometry. Again, this may be due to the uptake of thiocyanate anions by the brush, which will increase its inherent hydrophilicity by effectively charging the brush.

The variation in the determined LCST for the three techniques is clearly evident in Figure 4, where the calculated LCST values are plotted as a function of salt concentration. In the presence of potassium acetate the LCST decreases in an almost linear fashion with increasing salt concentration similar to results found by Jhon and co-workers for sodium chloride over this concentration range,⁴⁵ where the chloride anion is central to the Hofmeister series. The measured shift in LCST shown in Figure 4 was independent of the measurement technique indicating the kosmotropic salt affected brush thickness, rigidity and surface wettability equally. A notably different response is seen for potassium thiocyanate, where the LCST increased in the presence of the chaotropic salt. Interestingly, the measured LCST value in the presence of thiocyanate is dependent upon the measurement technique and this variation increases with ionic strength. This emphasises that a different mechanism is at play for the interaction of the pNIPAM brush with thiocyanate anions; as was discussed above in relation to Figure 3. Most probably the brush is becoming increasingly charged as the concentration of associated (bound) thiocyanate anions increases effectively increasing both the inter- and also intramolecular electrostatic repulsion between the pNIPAM chains and monomer units, respectively.³⁻⁵

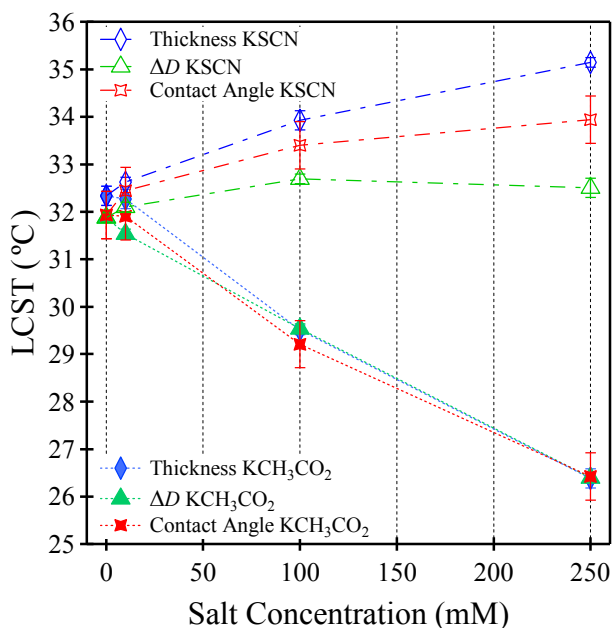


Figure 4. LCST values plotted as a function of salt concentration. The LCST in pure water was approximately 32 °C, as measured via the three techniques.

Figure 5 presents a schematic representation of the proposed differences in behaviour for a pNIPAM brush during the transition from a collapsed to swollen conformation (high to low T) in the presence of 250 mM potassium acetate or thiocyanate. The data in Figure 3a, b and c show that as the temperature was reduced below 28 °C in the presence of acetate (Figure 5a), the periphery of the brush became more soluble and extended normal to the substrate surface. At this point there is a measured increase in brush thickness and dissipation (brush started to swell and became more elastic) accompanied by a surface transition to a more hydrophilic state (Figure 5b). As the temperature was further reduced to ~23 °C, the brush thickness and dissipation continued to increase (Figure 5c), though wettability was already at equilibrium, until finally reaching a fully swollen conformation at ~20 °C (Figure 5d).

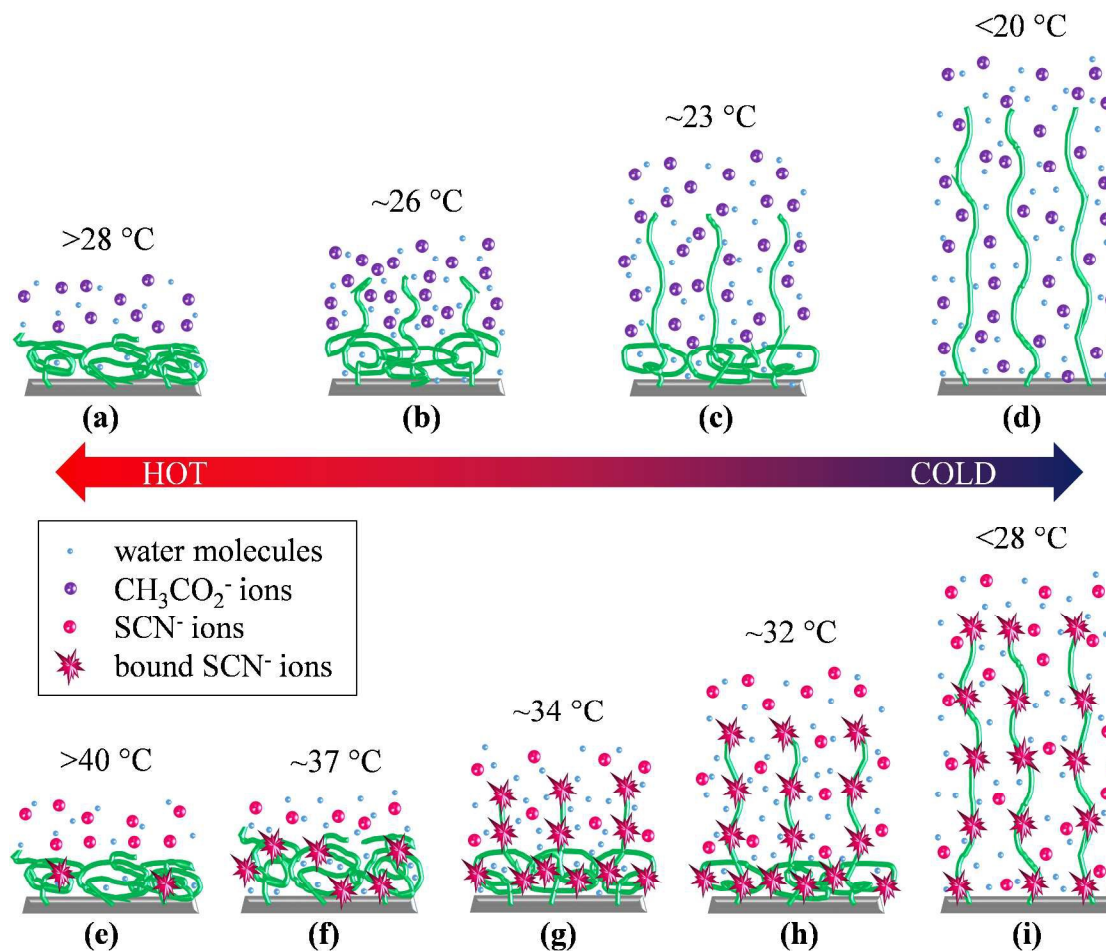


Figure 5. Schematic representation of the proposed equilibrium interactions between a pNIPAM brush and (a-d) 250 mM acetate ions and (e-i) 250 mM thiocyanate ions as a function of reducing temperature.

Based on the data shown in Figure 3d, e and f, the thermoresponse of the pNIPAM brush in the presence of 250 mM potassium thiocyanate is illustrated in Figure 5e-i. Firstly at high temperature, the solvated thickness of the collapsed pNIPAM brush layer slightly increases with thiocyanate concentration up to 250 mM; this is in contrast to the behaviour of the brush in the presence of acetate ions. This behaviour was not observed for the dissipation and contact angle measurements. This implies that while the pNIPAM brush starts to swell by solvent uptake below $\sim 38\text{ }^{\circ}\text{C}$, the rigidity and hydrophobicity of the brush remains unchanged. We propose that this is the result of a slight electrostatic repulsion within the brush layer caused by bound thiocyanate anions which partition within the collapsed brush (as discussed above). As the temperature is lowered further, by $\sim 34\text{ }^{\circ}\text{C}$ (Figure 5g) the periphery of the brush transitions to a more hydrophilic state accompanied by a further increase in brush thickness and minimal change

in rigidity. This suggests that the intra and inter-chain repulsion from the bound thiocyanate ions is strong enough to minimise any elastic behaviour from the soluble constituent of the polymer chains which are now extending normal to the surface into solution. As the temperature was reduced further (~ 32 °C, Figure 5h), the brush thickness continues to increase and now the soluble component of the polymer chains extend far enough from the substrate that they begin to increase in elasticity. As the temperature was reduced further, the brush thickness and dissipation continued to increase until the brush attained its fully swollen state at approximately 28 °C (Figure 5i).

Conclusions

By utilising a combination of in situ ellipsometry, QCM and static contact angle measurements, the equilibrium thermoresponse of pNIPAM brushes has been elucidated. Measurements were performed in pure water and salt solutions of different anion identity; with specific anion effects observed in the presence of potassium acetate and potassium thiocyanate. In all solution conditions the bulk brush behaviour, thickness and changes in dissipation, exhibited a broad swelling transition spanning approximately 15 °C from a collapsed and rigid conformation (high temperatures) to a more swollen and more elastic conformation (low temperatures). In contrast, the brush surface wettability changed over a narrow temperature range (~ 2 °C) which occurred at a relatively high temperature where the brush was still significantly collapsed and rigid. In pure water the measured LCST values were very similar (within 0.4 °C) for each technique employed. Kosmotropic acetate anions were shown to linearly reduce the LCST of the pNIPAM brushes with increasing ionic strength between 10 and 250 mM. Conversely, with increasing concentrations of the chaotropic thiocyanate anions, the LCST was shown to incrementally increase in the ellipsometry and contact angle experiments while the dissipation LCST measurements initially increased before plateauing at 100 mM. The thickness of the pNIPAM brush layer was seen to progressively increase with increasing potassium thiocyanate ionic strength at all temperatures. There was a significant difference in LCST between the three measurement techniques utilised for potassium thiocyanate, which increased at higher concentrations and became particularly evident at 250 mM. These phenomena are evidence that the specific ion effect that thiocyanate anions have on the hydration transition of pNIPAM

brushes follows a different mechanism to that observed in the presence of acetate anions. It is proposed that specific ion binding occurs between the thiocyanate anions and the amide moieties along the pNIPAM chains. Consequently, this process increases the electrostatic intra- and intermolecular repulsion within and between pNIPAM chains allowing the brush to begin to swell at higher temperatures and overall to a greater extent.

Acknowledgements

This research was supported by the Australian Research Council (DP110100041).

†Electronic Supplementary Information (ESI) available: wafer and QCM sensor preparation, pNIPAM brush synthesis details, ellipsometric data fitting protocol and optical model, polymerisation growth kinetics, as well as sigmoidal fit parameters for all experiments with an example figure defining each parameter.

References

1. W. Kunz, J. Henle and B. W. Ninham, *Curr. Opin. Colloid Interface Sci.*, 2004, 9, 19-37.
2. P. Lo Nostro and B. W. Ninham, *Chem. Rev.*, 2012, 112, 2286-2322.
3. Y. Zhang and P. S. Cremer, *Annu. Rev. Phys. Chem.*, 2010, 61, 63-83.
4. Y. Zhang, S. Furyk, D. E. Bergbreiter and P. S. Cremer, *J. Am. Chem. Soc.*, 2005, 127, 14505-14510.
5. I. Shechter, O. Ramon, I. Portnaya, Y. Paz and Y. D. Livney, *Macromolecules*, 2009, 43, 480-487.
6. F. Zhang, M. W. Skoda, R. M. Jacobs, D. G. Dressen, R. A. Martin, C. M. Martin, G. F. Clark, T. Lamkemeyer and F. Schreiber, *J. Phys. Chem. C*, 2009, 113, 4839-4847.
7. C. L. Henry and V. S. Craig, *Langmuir*, 2010, 26, 6478-6483.
8. A. Dér, L. Kelemen, L. Fábrián, S. Taneva, E. Fodor, T. Páli, A. Cupane, M. Cacace and J. Ramsden, *J. Phys. Chem. B*, 2007, 111, 5344-5350.
9. R. Freitag and F. Garret Flaudy, *Langmuir*, 2002, 18, 3434-3440.
10. H. D. B. Jenkins and Y. Marcus, *Chem. Rev.*, 1995, 95, 2695-2724.
11. L. M. Pegram and M. T. Record, *J. Phys. Chem. B*, 2007, 111, 5411-5417.
12. B. C. Gibb, *Isr. J. Chem.*, 2011, 51, 798-806.
13. L. Liu, Y. Shi, C. Liu, T. Wang, G. Liu and G. Zhang, *Soft matter*, 2014, 10, 2856-2862.
14. K. D. Collins, *Methods*, 2004, 34, 300-311.
15. P. Jungwirth and D. J. Tobias, *Chem. Rev.*, 2006, 106, 1259-1281.
16. L. M. Pegram and M. T. Record, *Proc. Natl. Acad. Sci. U.S.A.*, 2006, 103, 14278-14281.

17. S. Ghosal, J. C. Hemminger, H. Bluhm, B. S. Mun, E. L. Hebenstreit, G. Ketteler, D. F. Ogletree, F. G. Requejo and M. Salmeron, *Science*, 2005, 307, 563-566.
18. Y. Marcus, *Chem. Rev.*, 2009, 109, 1346-1370.
19. Y. Xia, N. A. Burke and H. D. Stöver, *Macromolecules*, 2006, 39, 2275-2283.
20. H. Schild, *Prog. Polym. Sci.*, 1992, 17, 163-249.
21. T. Patel, G. Ghosh, S. i. Yusa and P. Bahadur, *J. Dispersion Sci. Technol.*, 2011, 32, 1111-1118.
22. M. Boström, D. Williams and B. W. Ninham, *Biophys. J.*, 2003, 85, 686-694.
23. J. Paterová, K. B. Rembert, J. Heyda, Y. Kurra, H. I. Okur, W. R. Liu, C. Hilty, P. S. Cremer and P. Jungwirth, *J. Phys. Chem. B*, 2013, 117, 8150-8158.
24. K. B. Rembert, J. Paterová, J. Heyda, C. Hilty, P. Jungwirth and P. S. Cremer, *J. Am. Chem. Soc.*, 2012, 134, 10039-10046.
25. C. L. Gibb and B. C. Gibb, *J. Am. Chem. Soc.*, 2011, 133, 7344-7347.
26. C. L. Gibb, E. E. Oertling, S. Velaga and B. C. Gibb, *J. Phys. Chem. B*, 2015, 119, 5624-5638.
27. N. I. Abu-Lail, M. Kaholek, B. LaMattina, R. L. Clark and S. Zauscher, *Sensor Actuat. B-Chem*, 2006, 114, 371-378.
28. Y. Akiyama, A. Kikuchi, M. Yamato and T. Okano, *Langmuir*, 2004, 20, 5506-5511.
29. D. Cunliffe, C. de las Heras Alarcón, V. Peters, J. R. Smith and C. Alexander, *Langmuir*, 2003, 19, 2888-2899.
30. J. Kobayashi, A. Kikuchi, K. Sakai and T. Okano, *Anal. Chem.*, 2001, 73, 2027-2033.
31. B. Voit, D. Schmaljohann, S. Gramm, M. Nitschke and C. Werner, *Int. J. Mater. Res.*, 2007, 98, 646-650.
32. L. Ionov, M. Stamm and S. Diez, *Nano Lett.*, 2006, 6, 1982-1987.
33. D. Duracher, A. Elaïssari, F. Mallet and C. Pichot, *Langmuir*, 2000, 16, 9002-9008.
34. S. Balamurugan, S. Mendez, S. S. Balamurugan, M. J. O'Brie and G. P. López, *Langmuir*, 2003, 19, 2545-2549.
35. W. J. Brittain and S. Minko, *J. Polym. Sci., Part A: Polym. Chem.*, 2007, 45, 3505-3512.
36. N. Ishida and S. Biggs, *Macromolecules*, 2010, 43, 7269-7276.
37. E. S. Kooij, X. Sui, M. A. Hempenius, H. J. Zandvliet and G. J. Vancso, *J. Phys. Chem. B*, 2012, 116, 9261-9268.
38. K. Matyjaszewski, H. Dong, W. Jakubowski, J. Pietrasik and A. Kusumo, *Langmuir*, 2007, 23, 4528-4531.
39. J. D. Willott, T. J. Murdoch, B. A. Humphreys, S. Edmondson, G. B. Webber and E. J. Wanless, *Langmuir*, 2014, 30, 1827-1836.
40. J. D. Willott, T. J. Murdoch, B. A. Humphreys, S. Edmondson, E. J. Wanless and G. B. Webber, *Langmuir*, 2015, 31, 3707-3717.
41. J. D. Willott, B. A. Humphreys, T. J. Murdoch, S. Edmondson, G. B. Webber and E. J. Wanless, *Phys. Chem. Chem. Phys.*, 2015, 17, 3880-3890.
42. W. Ogieglo, *In-situ spectroscopic ellipsometry for studies of thin films and membranes*, Universiteit Twente Enschede, 2014.
43. G. Zhang, *Macromolecules*, 2004, 37, 6553-6557.
44. S. Varma, L. Bureau and D. Débarre, *arXiv:1511.07391v1 [cond-mat.soft]*, 2015.
45. Y. K. Jhon, R. R. Bhat, C. Jeong, O. J. Rojas, I. Szleifer and J. Genzer, *Macromol. Rapid Commun.*, 2006, 27, 697-701.
46. S. E. Moya and J. Irigoyen, *J. Polym. Sci., Part B: Polym. Phys.*, 2013, 51, 1068-1072.
47. I. Reviakine, D. Johannsmann and R. P. Richter, *Anal. Chem.*, 2011, 83, 8838-8848.
48. G. Sauerbrey, *J. Physik*, 1959, 155, 206-212.
49. C. Steinem and A. Janshoff, *Piezoelectric sensors*, Springer Science & Business Media 2007.
50. E. Bittrich, S. Burkert, M. Müller, K. J. Eichhorn, M. Stamm and P. Uhlmann, *Langmuir*, 2012, 28, 3439-3448.
51. T. Wang, Y. Long, L. Liu, X. Wang, V. S. Craig, G. Zhang and G. Liu, *Langmuir*, 2014, 30, 12850-12859.

52. P. Mason, G. Neilson, C. Dempsey, A. Barnes and J. Cruickshank, *Proc. Natl. Acad. Sci. U.S.A.*, 2003, 100, 4557-4561.